

1 **Aggregation and charge reversal of humic substances in the presence of**
2 **hydrophobic monovalent counter-ions: effect of hydrophobicity of humic**
3 **substances**

4 Azizul Hakim^{1,2}, and Motoyoshi Kobayashi ^{3,*}

- 5 1. Graduate School of Life and Environmental Sciences, University of Tsukuba, 1-1-1
6 Tennoudai, Tsukuba, Ibaraki 305-8572, Japan
- 7 2. Department of Soil Science, University of Chittagong, Chittagong-4331, Bangladesh
- 8 3. Faculty of Life and Environmental Sciences, University of Tsukuba, 1-1-1 Tennoudai,
9 Tsukuba, Ibaraki 305-8572, Japan

10 *Corresponding author, email: kobayashi.moto.fp@u.tsukuba.ac.jp

Abstract

11
12
13
14
15
16
17
18
19
20
21
22
23
24
25
26
27
28
29
30
31

To investigate the effect of hydrophobicity of humic substances (HSs) on their charging and aggregation, we studied the electrophoretic mobility and aggregation-dispersion of HSs in the presence of hydrophobic monovalent cations, namely, tetraphenylphosphonium TPP^+ . The used HSs were standard Suwannee river fulvic acid (SRFA), Suwannee river humic acid (SRHA), and Leonardite humic acid (LHA) with different contents of aromatic carbons. All of the HSs in the presence of TPP^+ showed charge reversal. The charge reversal pH or iso-electric point (IEP) of LHA was higher than that of SRFA and SRHA in every concentrations of TPP^+ , demonstrating the strong hydrophobic interaction between HSs, especially LHA, and TPP^+ . We also found that the formation of large visible aggregates of all the HSs at lower pH in the presence of TPP^+ . Large HS aggregates were markedly formed for LHA, manifesting the existence of stronger hydrophobic attraction among LHAs with TPP^+ . The appearance of aggregates of all the HSs with TPP^+ was confirmed by microscopic observation and the size determination by dynamic light scattering. The HS aggregates showed fractal structure. The values of fractal dimension D_f of HS aggregates were 2-2.2 in quiescent conditions, indicating that the HS aggregates with TPP^+ were formed via cluster-cluster aggregation with restructuring. The D_f increased to 2.8-2.9 in stirring conditions, implying that the compact aggregates were formed through the continuous aggregate breakage and the regrowth between smaller aggregates and larger aggregates.

Keywords: humic substances, charge reversal, aggregation-dispersion, hydrophobicity

32 **Introduction**

33 Humic substances (HSs) are considered as one of the most important sources or sink of
34 organic carbons in soil and water environments [1] and play a vital role in nutrient cycling, and
35 the fate and transport of pollutants [2]. The surface active binding sites and highly reactive
36 nature of HSs [3] influence the binding of organic and inorganic contaminants and also affect
37 the bioavailability of metal ions and mobility in soil environment [4]. Some previous studies
38 specially highlight on the structural heterogeneity and the molecular conformation such as
39 supramolecular and self-assembly [5-8], fractal aggregate [9-13], and spherocolloids, [14].
40 Some studies on the adsorption of humic substances on minerals surfaces [15] and aggregates
41 formation [16] were carried out. The charging and aggregation behaviors of minerals particles
42 and nanoparticles [17-20] with humic substances were also investigated. Nevertheless, there
43 are scanty data on the structure of humic substances aggregates and the charge reversal of
44 humic substances itself as natural colloids. A recent study on humic acid co-precipitation with
45 ferrihydrite discussed about the unlikeliness of the humic acid used as a model colloid, though
46 the use of humic acid as network of linear macromolecules and large colloids is more consistent
47 [21].

48 Humic substances with Ca^{2+} , lysozyme, surfactants, and polymer can be aggregated to form
49 large visible and settleable aggregates [4, 22, 23], which are crucially important for the fate
50 and separation of HSs with chemicals. Generally aggregation and dispersion of colloidal
51 particles is discussed on the basis of Derjaguin, Landau, Verwey and Overbeek (DLVO) theory,
52 which assumes that the interparticle interaction is given as the sum of van der Waals and
53 electrostatic interactions. The latter interaction is influenced by the electric charge of particles.
54 The aggregation usually occurs at the condition where the net charge becomes zero. Such
55 condition is called charge neutralization detected as an iso-electric point obtained from

56 electrophoresis. The charge neutralization is often realized by the adsorption of appropriate
57 amount of oppositely charged ionic substances such as polymers, surfactants, and proteins. The
58 bindings and adsorption of metal ions depend on different factors such as pH, humic
59 concentration, types of humic substances, ionic strength, temperature, ternary complexes
60 formation, etc [24]. The binding of cationic surfactants to humic acid was observed due to the
61 combined effect of electrostatic and hydrophobic interactions, whereas no notable binding was
62 observed between anionic surfactants and humic acid [25]. In some cases the overdose of
63 absorbable ionic substances induces charge reversal. Screening of electrostatic interaction and
64 charge reversal are observed by the addition of various amounts of polyelectrolyte and
65 oppositely charged ion as influenced by the amount of adsorption. Several recent researches
66 report that the hydrophobic interaction plays an important role in charge reversal and/or charge
67 neutralization for different natural and synthetic colloids and biomaterials [26-31].

68 In addition to the DLVO interaction, some other forces and interactions such as the
69 hydrophobic interactions [22, 23, 26-31], hydrogen bonding [32, 33], hydration forces [34, 35],
70 and depletion interactions [36] are recognized to play an important role in aggregation-
71 dispersion of colloid particles in different environmental systems. Humic substances from
72 different sources show the aggregation and sedimentation behaviors in the presence of
73 inorganic salts, organic surfactants, proteins and enzymes [22, 23, 27, 37]. Nevertheless, the
74 mechanisms behind the aggregation and charging behaviors of humic substances in the
75 presence of adsorbing ions are still vague. Therefore, the research on the fundamental colloidal
76 behavior of humic substances is still important in the field of natural colloids.

77 Big hydrophobic ions, such as tetraphenylboron, tetraphenylarsonium, and
78 tetraphenylphosphonium, are used to modify the interfacial properties of clay colloids [38, 39]
79 and to monitor permeability and interaction of the lipid membranes and biological cells [40,
80 41]. Recently, big hydrophobic tetraphenylboron anions and tetraphenylarsonium cations are

81 also selected as tracers to study the extent of hydrophobicity of typical proteins [42]. While it
82 is inferred that the hydrophobicity of humic substances plays crucial roles in the adsorption
83 and aggregation, the interaction of humic substances with such big hydrophobic ions have
84 never been reported.

85 In this context, we came up with performing the study on the influence of hydrophobic
86 tetraphenylphosphonium (TPP) cations on the behaviors of humic substances. We found that
87 TPP significantly affects the aggregation and charge reversal of three different humic
88 substances with different hydrophobicity. In this paper, we report the result of the study on the
89 electrophoretic mobility and aggregation behaviors of the humic substances with TPP in
90 different concentration and pH of the solution. To the best of the authors' knowledge, our
91 results are the first mobility data demonstrating the charge reversal of humic substances itself
92 and thus are of novelty. We expect that the results obtained in this research can be generalized
93 to the study of the removal of hydrophobic pollutants and aggregation-dispersion of HSs with
94 hydrophobic organic pollutants such as dyes and drugs.

95 **Experimental**

96 **Materials**

97 Three humic substances (Suwannee river fulvic acid, Suwannee river humic acid and
98 Leonardite humic acid) from International Humic Substances Society (IHSS) were used as
99 natural organic matters in this study. These are referred to as SRFA, SRHA, and LHA hereafter.
100 The primary stock solutions of the humic substances were prepared by dissolving solid samples
101 to KOH solution (Wako Pure Chemical Industries) containing base equivalent or more than the
102 amount of carboxylic acid groups of each humic substance. Before dissolving the solid sample
103 to KOH solutions, the supplied samples were oven-dried at 65°C overnight to reduce moisture.
104 After dissolving solid humic substances to KOH solutions, the suspension (wt. %) were stirred

105 overnight, then the secondary standard solutions were prepared by dilution with deionized
106 water (Elix, Millipore) to a concentration 500 mg/L. The pH values of the secondary standard
107 solutions of humic substances were around neutral (6.5-7.2). The concentration of humic
108 substances (HSs) was maintained at 50 mg/L in every measurement in this study. Some of the
109 parameters of the HSs from IHSS are listed in Table 1. The HSs used in this research were
110 chosen depending on their charge groups and hydrophobicity differences based on their carbon
111 content and aromaticity.

112 The electrolytes of simple KCl (JIS special grade, Wako Pure Chemical Industries) and
113 hydrophobic tetraphenylphosphonium chloride (TPPCL) (EP grade, Tokyo Chemical Industry
114 Co.) were used to examine the effect of hydrophobic ions. The salt concentrations were from
115 10 mM to 100 mM. The pH was controlled by using HCl (Wako Pure Chemical Industries) or
116 KOH. Carbonate free KOH solutions were prepared by following the method described in ref.
117 [43]. The salt solutions were filtered (DISMIC 25HP 0.2 μm , ADVANTEC) in every new
118 preparations. All the solutions of this study were degassed under reduced pressure (GCD-051X,
119 ULVAC) to avoid the CO₂ contamination prior to our experiments.

120 **Methods**

121 Electrophoretic mobility measurements

122 The electrophoretic mobilities of the three humic substances (HSs) were measured in the
123 presence of both KCl and tetraphenylphosphonium chloride (TPPCL) at 20 °C with a Zetasizer
124 Nano ZS apparatus (Malvern Instruments). The electrophoretic mobility measurements were
125 carried out as a function of salt concentration of KCl and TPPCL. The KCl of 10 mM and 50
126 mM and the TPPCL of 10 mM, 50 mM, and 100 mM were used as a function of pH (3-10). For
127 each condition of salt concentration, the measurements were reproduced and every experiment
128 was done at least two times and we got similar data. For the measurements of electrophoretic
129 mobility, all secondary standard solutions of humic substances were sonicated one-time for 20

130 minutes before mixing with water, salts (TPPCL) and KOH/HCl. The concentration of humic
131 substances (SRFA, SRHA, and LHA) was maintained at 50 mg/L. The pH values of the
132 suspension of each measurement were checked by a combination electrode (ELP-035, TOA-
133 DKK).

134 Macroscopic and microscopic observation of aggregation and dispersion

135 Visual observations of aggregates of humic substances (SRHA, SRFA, and LHA) in TPPCL
136 solutions were performed at 50 mM of TPPCL with 50 mg/L of humic substances of each type
137 as a function of pH for 24 hours. A series of 5 mL suspensions of 50 mg/L humic substances
138 in 50 mM of TPPCL at pH 3-10 was prepared in the prewashed and screw-capped polystyrene
139 bottles and left stand for 24 hours. The pH was controlled by the addition of KOH and HCl. It
140 was hard to definitely control the sharp pH value at each cases of the experimental
141 measurement because of the protonation and de-protonation of humic substances at various pH.
142 The macroscopic pictures and videos (see supporting information) of the suspensions after 24
143 hours were taken for visual confirmation of the formation of aggregates.

144 After 24 hours later, the aggregated and dispersed suspensions of humic substances in
145 TPPCL were observed under a microscope for a range of pH from 3 to 9. This microscopic
146 study was performed to evaluate the tentative size and arrangements of aggregates of humic
147 substances with TPPCL salts. The microscope used in this study was Shimadzu BA210E,
148 Moticam 580INT.

149 Dynamic light scattering

150 The size of the particles and/or aggregates of humic substances in TPPCL was determined by
151 dynamic light scattering (DLS) technique applying backscattering detection (173° detection
152 optics) at 20 °C with a Zetasizer Nano ZS apparatus (Malvern Instruments). Cleaned disposable
153 cuvettes containing 1 mL of sample were used in every measurement of DLS. The sample
154 suspensions of humic substances with TPPCL in the cuvettes were briefly sonicated for 2

155 minutes after mixing, and then the measurements for DLS just started after 5 minutes from the
156 mixing. After measurements started, it took times for temperature equilibrium at 20°C and for
157 the optimization of optical condition. Each measurement consisted of 5 runs and the duration
158 of each run was 10 s.

159 Aggregate structure analysis

160 For the aggregates of humic substances (50 mg/L) formed with 50 mM TPPCl, a structural
161 analysis was performed. For the purpose of aggregates structure analysis, the determination of
162 fractal dimension of aggregates was carried out by small angle light scattering using SALD
163 2300 (SHIMDZU), by which the relation of scattered light intensity I with scattering angle, is
164 obtained. In the medium of suspension, the magnitude of the incident and scattered wave
165 vectors difference of light, a scattering vector, is denoted as Q , and the Q is expressed as the
166 following equation (1)

167

$$168 \quad Q = \frac{4\pi n \sin\left(\frac{\theta}{2}\right)}{\lambda} \quad (1)$$

169

170 where n is the refractive index of the suspending medium, θ is the scattering angle, and λ is
171 the wavelength of the laser light in a vacuum. The fractal dimension D_f is determined as the
172 relation of I and Q for scattering aggregates. That is, relation among I , Q and D_f is expressed
173 as (2)

174

$$175 \quad I \propto Q^{-D_f} \quad (2)$$

176

177 Thus, the log-log scale plot of I against Q , with the power law relationships yields a straight
178 line in a fractal regime. The slope of this straight line is used as fractal dimension D_f in this
179 study. Measurements were carried out after mixing of the suspension at pH 3 as a function of

180 different time intervals. The experiment for aggregates structure analysis was carried out no
181 stirring and upon stirring conditions in a batch cell of SALD 2300 (SHIMDZU) using 12 mL
182 of solutions in every set-up.

183 Table 1. Some selected composition of the three humic substances reported by IHSS.

IHSS samples	Carbon content % (w/w)	Carboxylic groups (meq/g-C)	Phenolic groups (meq/g-C)	Aromatic carbon (peak area percentages) (165-110 ppm)
SRFA II (Suwannee river fulvic acid)	52.34	11.17	2.84	22
SRHA II (Suwannee river humic acid)	52.63	9.13	3.72	31
LHA (Leonardite humic acid)	63.81	7.46	2.31	58

184

185 **Results and Discussion**

186 Electrophoretic mobility in KCl

187 The electrophoretic mobility of three HSs (SRFA, SRHA, and LHA) in the presence of KCl
188 at various pH values are presented in the supporting information. Electrophoretic mobility is
189 presented with the difference of hydrophobicity (Table 1) of these three humic substances at
190 10 mM and 50 mM KCl concentrations (see supporting information). All the values of mobility
191 of HS in KCl solution are negative and thus we observe no charge reversal of HSs in the KCl
192 solution.

193 Electrophoretic mobility of HSs in the presence of TPPCl

194 The electrophoretic mobility of humic substances in the presence of hydrophobic
195 tetraphenyl phosphonium chloride (TPPCL) at the pH range 3-10 in 10 mM, 50 mM and 100 mM
196 of TPPCl concentrations is presented in Fig. 1. We find the obvious charge reversal for all three
197 humic substances (SRFA, SRHA, and LHA) at every concentrations of TPPCl (10 mM, 50
198 mM, and 100 mM) as demonstrated in Fig. 1. The charge reversal is probably induced by
199 hydrophobic interactions between TPP⁺ and HSs as inferred from the result in earlier literature
200 for well-characterized colloidal particles; hydrophobic ions give rise to the charge reversal of
201 hydrophobic colloids [26, 29, 30, 44, and 46]. The results indicate that all the HSs are
202 hydrophobic in nature, while FA is well-dissolved in water at all pH. This is because
203 hydrophobic resin is used to collect FA, meaning that rather hydrophobic fraction of dissolved
204 natural organic matter at all pH can be collected as fulvic acid.

205 The pH where the charge reversal occurs or the iso-electric point (IEP) of these HSs
206 increases with the increase in TPPCl concentration (Fig. 1). The IEP also shifts towards higher
207 pH values with the increase of hydrophobicity or aromaticity (hydrophobicity:
208 LHA>SRHA>SRFA, see Table 1). At low TPPCl concentration (10 mM), the IEP for SRFA
209 and SRHA is around pH 3 and it is around pH 4 for LHA. The higher the hydrophobicity is,
210 the higher the pH of the charge reversal point is. The result indicates more hydrophobic
211 interaction prevails in the case of LHA with TPPCl than that of SRFA and/or SRHA with
212 TPPCl.

213 In the presence of TPPCl, the pH range of charge reversal of LHA is more than that of SRFA
214 and SRHA (Fig. 1 A- Fig. 1 C). The IEPs or charge reversal points for LHA are around pH 4,
215 pH 6 and pH 7, which are higher than those of SRFA and/or SRHA at pH around 3, 5 and 6 in
216 10 mM, 50 mM and 100 mM TPPCl, respectively. Hyuang and Kim [45] reported that HSs
217 with higher content of aromatic groups adsorb more on hydrophobic carbon nanotubes. Thus,

218 Figure 1 provides the evidence of strong hydrophobicity of LHA. Hakim et al. [26] and
219 Sugimoto et al. [46] suggest that hydrophobic interaction is strong for weakly charged surface.
220 This suggestion is supported by the data in Figure 1. That is, the charge reversal occurs at low
221 pH, where HSs are weakly charged. An investigation on the interaction of humate and
222 cetyltrimethylammonium (CTAB) confirmed the formation of humate-CTAB complex and the
223 occurrence of charge neutralization and charge reversal by electrostatic and hydrophobic
224 interactions [47]. These results also support our study.

225 Figure 1 shows that the absolute value of electrophoretic mobility decreases with the
226 increase of TPPCl concentrations (10 mM-100 mM) at the pH range (7-10). This reduction
227 could be explained by the compensation of surface charge by the adsorption of TPPCl on humic
228 substances. The charge reversal points, where the positive electrophoretic mobility of HSs
229 reverses to negative mobility increases with the increase in TPPCl concentration from 10 mM
230 to 50 mM. At pH 7-10 at 10 mM and 50 mM of TPPCl, however, the magnitude of mobility
231 decreases. While this reduction is probably related to the change in conformation of HSs and
232 ion distribution around HSs, the quantitative description is still difficult. Many studies reported
233 the zeta potential and electrophoretic mobility of humic substances specifying no inversion of
234 charges in different mono and divalent electrolytes solutions [4, 33, and 48]. The
235 electrophoretic mobility of these three humic substances in KCl solutions measured in this
236 study show no reversal of charges of humic substances (see supporting information),
237 supporting the previous literature. It should be noted that, to the best of the authors' knowledge,
238 this paper reports the first data on electrophoretic mobility showing the charge reversal of
239 humic substances and concurrent relations with aggregation as a factor of hydrophobic
240 interactions.

241

242

243 Macroscopic and microscopic observations of HSs aggregates formation with TPPCl

244 We performed the visual observation of aggregation and dispersion of humic substances
245 (SRFA, SRHA, and LHA) in tetraphenylphosphonium chloride (TPPCL) solutions at 50 mM
246 as a function of pH after 24 hours (Photograph 1). We observed large ramified and interlinked
247 aggregates of the HSs with TPPCl (Photograph 1 A, B, C) at pH around 3-5 for SRFA and
248 SRHA and pH around 3-7 for LHA. The stronger network formation of large aggregates of
249 LHAs at low pH can allow aggregates of LHAs withstand sedimentation. The videos of
250 macroscopic observation at low pH confirm the strong interconnections and ramification of the
251 HSs aggregates (see supporting information videos S1 –S5). Smaller size aggregates were also
252 observed in the pH around 6 in the case of SRFA and SRHA. These smaller and mostly
253 deposited aggregates, that were not large and ramified like the pH around 3-5, were more
254 obvious in the case of SRHA. In the case of LHA at higher pH (7-10), smaller settled aggregates
255 were also observed and those were not large ramified and strongly interconnected. Therefore,
256 the sediment is clearly seen. We see clear views showing that the interconnection and size of
257 aggregates decrease with the increase in pH for the HSs-TPPCL suspension. At higher pH
258 values (7-10), the SRFA and SRHA were more dispersed probably due to weak hydrogen bond
259 and weak hydrophobic interaction or the domination of electrostatic repulsion over the
260 attractive interactions with TPPCl and/or humic substances itself. This qualitative observation
261 of aggregates formation has some limitations due to manual handling and observation by naked
262 eye.

263 These complex and interlinked aggregates are related to the change of electrophoretic
264 mobility with pH as described in the previous section. Avena and Wilkinson [49] pointed out
265 the importance of the hydrophobic interaction and hydrogen bond for the interaction of humic
266 substances. The probable causes behind the formation of large aggregates are due to the
267 existence of hydrophobic interactions [50]. This rather strong connection at low pH (3-5)

268 makes it possible that the aggregates withstand the force of gravity in the medium and the
269 sedimentation is inhibited [51].

270 The microscopic observation was also performed for the confirmation of behavior and
271 nature of aggregates. In photographs 2, 3, and 4, the structural arrangements and tentative size
272 of the aggregates can be seen. The photographs 2, 3, and 4 show the aggregates formed at
273 different pH from 3-9 in 50 mM TPPCl after 24 hours from the mixing. These microscopic
274 photographs depict the verification of the existence of aggregates with interconnection among
275 the particles in low pH of SRFA and SRHA. The LHA shows aggregation at all pH with a
276 decreasing trend of size with pH, although there were some limitations in the microscopic study.
277 With the increase of hydrophobicity (SRFA<SRHA<LHA), larger and concentrated aggregates
278 appeared from photographs 2 to 4. The photographs 2, 3, and 4 of optical microscopy show
279 some smaller units and some large units at pH around 3, and the large aggregates units look to
280 be formed through the repetition and self-assembly of smaller units. At higher pH value, the
281 SRFA and SRHA show no larger aggregate units in the photographs 2 and 3 even though at
282 higher magnification, although LHA shows large aggregates in the higher range of pH. This
283 result indicates the higher hydrophobicity triggered the aggregation. The repetition and
284 rearrangements of the aggregates manifest the hierarchical architecture of the aggregates
285 reported in the previous study [4, 9]. Some authors found similar structural natures and
286 arrangements of humic acid aggregates with CaCl₂ in different magnification of optical
287 microscope [52] and transmission electron microscopy studies. During the microscopic
288 observation of the aggregates in this research, we observed the motion of some aggregates as
289 a moving unit by Brownian motion of the aggregates. Such motion was also reported in the
290 earlier study [4]. The motion of the aggregates can also be due to fluid flow and sedimentation
291 due to gravity in the medium.

292

293 Dynamic light scattering (DLS) and aggregates size

294 To characterize the pH dependence of the aggregation, the DLS measurements of HSs
295 aggregates in TPPCl solutions were carried out. Figure 2 shows that the hydrodynamic Z-
296 average diameter of HSs is around 1200-1600 nm at pH 3-4 for SRFA and SRHA with a single
297 discrete value of Z-average diameter higher than this and at pH 3-5 for LHA, indicating that
298 the formation of HS aggregates in the presence of TPPCl. The DLS results are consistent with
299 those by the visual observation described above in the presence of TPPCl. Generally, the
300 aggregation of colloidal particles occurs around IEP. Our results, however, deviate from this
301 general rule. Probably, hydrophobic interaction is the driving mechanism of TPP-induced
302 aggregation. That is, the presence of TPP⁺ ions induces the aggregation of HSs by increasing
303 the hydrophobicity of HSs, and thus enhances the formation of HS aggregates through the
304 increased tendency of HSs escaping from the water. The largest aggregates size around 2300
305 nm was found for LHA at pH 3-4. At every pH values, the sizes of aggregates of LHA with
306 TPPCl are larger than that of SRFA and SRHA with TPPCl. The DLS results manifest the
307 highest hydrophobicity and the evidence of stronger hydrophobic interaction for LHA. On the
308 contrary, the aggregates size of HSs with 50 mM TPPCl decreases with increasing pH in every
309 type of HSs (SRFA, SRHA, and LHA) as expected from the visual observation. At low pH,
310 less ionization of surface charging groups, the COOH and –OH causes more hydrophobic
311 interaction between HSs and TPPCl. Furthermore, at low pH, the HSs aggregates are formed
312 by hydrophobic interaction, hydrogen bonding, and probably some charge-patch attraction. At
313 high pH, the electrostatic repulsion and weak hydrophobic interaction among HSs predominate
314 and thus hinder the formation of the larger size of aggregates. In addition we focused on the
315 formation of aggregates and concentrated the effect of hydrophobicity which provoke us to use
316 different HSs with varying hydrophobicity regardless the size of primary humic substances. It
317 was difficult to maintain the same size of primary particles varying with hydrophobicity in this

318 investigation. The decrease of the sizes of aggregates with pH indicating the electrostatic
319 repulsion at higher negative charge with increasing pH, lower aggregates size and less
320 hydrophobic interactions. The Z- average diameters of different humic substances with pH
321 variation in hydrophilic salts were studied in the previous researches conducted by different
322 groups. They found aggregates of humic acids larger than 1000 nm of Z-average diameter at
323 low pH [33, 53]. Another group found aggregates of humic acids larger than 1000 nm of
324 average hydrodynamic radius in NaCl and MgCl₂ at different concentration and time intervals
325 in pH around 3.6 and 7.1 [54]. The previous study [33] shows the decreasing tendency of size
326 at high pH due to the hindering of the H-bond and increasing of the electrostatic repulsion. The
327 larger size at low pH is probably due to the reduction of repulsion and the intermolecular H-
328 bonding. All our results confirm that the hydrophobic counter-ions TPP⁺ induce the
329 aggregation of humic substances and the degree of hydrophobicity influences the degree of
330 aggregation of HSs, LHA > SRHA > SRFA. It should be noted here that the Z-average diameter
331 of aggregates at low pH in this investigation shows higher values in DLS other than the
332 previous investigation performed in monovalent hydrophilic electrolytes solutions refer to a
333 hydrophobic interaction for larger aggregation.

334 Fractal dimension and aggregates structure analysis

335 The temporal change in fractal dimension D_f of the aggregates of HSs in 50 mM TPPCl at
336 pH 3 is shown in Fig. 3, where the effect of stirring is also demonstrated. In every cases, the
337 fractal dimension with stirring shows higher values than that of non-stirring condition. Clear
338 dependence of D_f on the type of HSs is not found. The values of fractal dimension of HSs are
339 2-2.31 at no stirring. On the contrary, the values of D_f of SRFA, SRHA and LHA are raised to
340 2.8, 2.88, and 2.87 at stirring condition (Fig. 3). The D_f values without stirring are reasonable
341 compared to the previous study. The fractal dimension of simulated flocs formed through
342 diffusion limited cluster-cluster aggregation is around 1.8, while the D_f around 2.1 can be

343 obtained by reaction limited cluster-cluster aggregation with restructuring [55]. From the
344 comparison of the simulation results with our data, HSs flocs with TPP are formed through
345 weaker contact forces allowing restructuring even at most aggregated state at low pH.

346 The values of fractal dimension with stirring are relatively higher than that by previous
347 studies for aggregates such as kaolin with alum [56], natural organic matters such as humic
348 acid with chitosan coagulants and Al species [57]. The Fe precipitates flocs showed a D_f value
349 2.6 after breakage [58], a modelling of viscosity for coagulated suspension showed D_f values
350 around 2.2 - 2.6 [59], and a comparative study of fractal dimension of humic acid flocs and
351 clay flocs showed higher fractal dimension of humic acid flocs (D_f around 2.7) than that of
352 clay flocs [60]. In this study, we found the higher value of D_f , indicating the more compact
353 structure of aggregates due to the stirring. Studies revealed that the polydispersity of primary
354 particles and aggregates cluster of TiO_2 aerosols, polystyrene latex, some polymers, and
355 hematite particles may have an impact on the compactness and subsequent fractal structure
356 [61-63]. From this situation in our case we measured the fractals at a fixed pH around 3, though
357 HSs are not totally monodisperse and this has some effect on fractals structure by influencing
358 the power law relation in a largely overlapping scattering exponent regimes between scattering
359 wave vector and scattering intensity. Considering this effect of polydispersity the fractals has
360 somehow influenced and had a higher value observed due to the presences of small and large
361 aggregates and particles in stirring condition. Hoekstra et al. [64] reported that D_f of 2.7 was
362 obtained for flocs formed in reaction limited regime under shear. Torres et al. [65] showed that
363 D_f increased to 2.9 through the collision between a single particle and a cluster in a shear flow.
364 Some recent researches reported high D_f value around 2.75 of chitosan coagulant for different
365 aluminium species in humic acid treatment [57], and D_f value almost 3.0 for polystyrene latex
366 floc induced by FeCl_3 , NaCl and $\text{Al}_2(\text{SO}_4)_3$ and found the increase of fractal dimension with
367 salt and particle concentrations [66]. The comparison of our data with previous studies

368 suggests that the repeated collision between the smaller HS aggregates and larger HS
369 aggregates during the breakage and re-growth under stirring produces TPP-induced HSs flocs
370 with higher values of the fractal dimension. This formation of aggregates may be due to the
371 cluster-cluster aggregation [56] with restructuring and/or penetration of small cluster or broken
372 aggregates fraction into the large aggregates structure.

373 The aggregation between a small cluster and large cluster, which can often happen in
374 sheared suspension at high particle concentration, might result in higher D_f . This is one of the
375 possible mechanisms of the present high D_f value. The penetration is also stimulated by soft
376 permeable structure [48] of humic substances. The aggregation of humic substances in stirring
377 condition caused by hydrophobic interaction and/or by charge neutralization with TPPCl
378 undergoes continuous collisions by fluid flow. Also the flow causes frequent collision and
379 irreversible penetration of some smaller aggregates in the permeable porous structure of HSs
380 aggregates. These processes make the HSs aggregates more compact in structure, and thus flocs
381 formed in shear flow have the compact structure [64, 67].

382

383 **Conclusion**

384 We found that the obvious charge reversal of all the humic substances (HSs) occurs in the
385 presence of hydrophobic cation TPP^+ and the iso-electric point (IEP) depends on the
386 hydrophobicity of HSs and TPP^+ concentration. The HSs form large visible aggregates in
387 TPPCl solution at low pH for SRFA and SRHA, and in all pH for LHA. The size of LHA
388 aggregates is also larger than those of SRFA and SRHA. The HS aggregates formed with TPP^+
389 have large size and fractal structure. This new findings of charge reversal and formation of
390 large HS aggregates in the presence of hydrophobic counter ion will definitely help us to partly
391 understand and may unfold a new arena of future research of humic substances. Our findings

392 are available to predict and depict the fate of various hydrophobic ions such as dyes and
393 medicines in soil and water environment.

394 **Conflict of interest**

395

396 The authors declare that they have no conflict of interest associated with this article.

397

398 **Acknowledgments**

399 The present work was financially supported by JSPS KAKENHI (15H04563 and 16H06382).

400 We would like to thank Mr. Tri Hoa Phan from Department of Chemistry, University of Iowa

401 for his great support during the experimental work.

402 **References**

- 403 [1] N. Senesi, E. Loffredo, The chemistry of soil organic matter, In: Spark, D.L., Ed., Soil
404 Physical Chemistry, CRC Press, Boca Raton (1999) 239-370.
- 405 [2] A. Piccolo, The Supramolecular Structure of Humic Substances, *Soil Sci.* 166 :11
406 (2001) 810–832. Doi: <https://doi.org/10.1097/00010694-200111000-00007>
- 407 [3] P. MacCarthy, The principles of humic substances, *Soil Sci.* 166 (2001) 738–751.
- 408 [4] N. Kloster, M. Brigante, G. Zanini, M. Avena, Aggregation Kinetics of humic acids in
409 the presence of Calcium ions, *Colloids and Surface A : Physicochem. Eng. Aspects* 427
410 (2013) 76-82
- 411 [5] P. Conte, A. Piccolo, Conformational arrangement of dissolved humic
412 substances. Influence of solution composition on association of humic molecules,
413 *Environ. Sci. Technol.* 33 (1999) 1682–1690.
- 414 [6] V. D’Orazio, N. Senesi, Spectroscopic properties of humic acids isolated from the
415 rhizosphere and bulk soil compartments and fractionated by size exclusion
416 chromatography, *Soil Biol. Biochem.* 41 (2009) 1775–1781.
- 417 [7] M. R. Esfahani, H. A. Stretz, M. J. M. Wells, Abiotic reversible self-assembly of fulvic
418 and humic acid aggregates in low electrolytic conductivity solutions by dynamic light
419 scattering and zeta potential investigation, *Sci. Total Environ.* 537 (2015) 81–92.
420 Doi:10.1016/j.scitotenv.2015.08.001.
- 421 [8] D. Šmejkalová, A. Piccolo, Aggregation and disaggregation of humic supramolecular
422 assemblies by NMR diffusion ordered spectroscopy (DOSY-NMR) *Environ. Sci.*
423 *Technol.* 42: 3 (2008) 699–706. Doi: 10.1021/es071828p

- 424 [9] G. Chilom, J. A. Rice, Structural organization of humic acid in the solid state, *Langmuir*
425 25:16 (2009) 9012–5. Doi:10.1021/la900750z.
- 426 [10] G. Chilom, A. Baglieri, C. A. Johnson-Edler, J. A. Rice, Hierarchical self-assembling
427 properties of natural organic matter's components, *Organic Geochemistry* 57 (2013)
428 119-126
- 429 [11] P. S. Redwood, J. R. Lead, R. M. Harrison, I. P. Jones, S. Stoll, Characterization of
430 humic substances by environmental scanning electron microscopy, *Environ. Sci.*
431 *Technol.* 39 (2005) 1962–1966.
- 432 [12] J. A. Rice, J. S. Lin, Fractal nature of humic materials, *Environ. Sci. Technol.* 27 (1993)
433 413–414.
- 434 [13] N. Senesi, Aggregation patterns and macromolecular morphology of humic
435 substances: a fractal approach, *Soil Sci.* 164:11 (1999) 841–856.
- 436 [14] K. Ghosh, M. Schnitzer, Macromolecular structures of humic substances, *Soil Sci.*
437 129: 5 (1980) 266–276.
- 438 [15] L. Weng, W. H. Van Riemsdijk, L. K. Koopal, T. Hiemstra, Adsorption of Humic
439 Substances on Goethite: Comparison between Humic Acids and Fulvic Acids, *Environ.*
440 *Sci. Technol.* 40 (2006) 7494-7500
- 441 [16] P. A. Maurice, K. Namjesnik-Dejanovic, Aggregates structures of sorbed humic
442 substances observed in aqueous solution, *Environ. Sci. Technol.* 33 (1999)
- 443 [17] M. Baalousha, Aggregation and disaggregation of iron oxide nanoparticles: influence
444 of partial concentration, pH and natural organic matter, *Science of the total environment*
445 407 (2009) 2093-2101, Doi:10.1016/j.scitotenv.2008.11.022

- 446 [18] M. Ren, H. Horn, F. H. Frimmel, Aggregation behavior of TiO₂ nanoparticles in
447 municipal effluents: influence of ionic strength and organic compounds, *Water*
448 *Research* 123 (2017) 678-686. Doi: <http://dx.doi.org/10.1016/j.watres.2017.07.021>
- 449 [19] R. F. Domingos, N. Tufenkji, K. J. Wilkinson, Aggregation of titanium dioxide
450 nanoparticles: Role of Fulvic Acid, *Environ. Sci. Technol.* 43: 5 (2009)
- 451 [20] T Abe, S. Kobayashi, M. Kobayashi, Aggregation of colloidal silica particles in the
452 presence of fulvic acid, humic acid, or alginate: effects of ionic composition, *Colloids*
453 *and Surfaces A: Physicochemical and Engineering Aspects* 379 :1 (2011) 21-26
- 454 [21] R. Angelico, A. Ceglie, H. Ji-Zheng, L Yu-Rong, G. Palumbo, C. Colombo, Particle
455 size, charge and colloidal stability of humic acids coprecipitated with Ferrihydrite,
456 *Chemosphere* 99 (2014) 239-247.
- 457 [22] W. F. Tan, L. K. Koopal, L. P. Weng, W. H. van Riemsdijk, W. Norde, Humic acid
458 protein complexation, *Geochimica et Cosmochimica Acta* 72: 8 (2008) 2090–2099.
459 Doi: <https://doi.org/10.1016/j.gca.2008.02.009>
- 460 [23] W. F. Tan, L. Koopal, W. Norde, Interaction between humic acid and lysozyme,
461 studied by dynamic light scattering and isothermal titration calorimetry, *Environ. Sci.*
462 *Technol.* 43: 3 (2009), 591–596. Doi: <https://doi.org/10.1021/es802387u>
- 463 [24] E. Tipping, Cation binding by humic substances, Cambridge University press (2002)
- 464 [25] L.K. Koopal, T.P. Goloub, T.A Davis, Binding of ionic surfactants to purified humic
465 acid, *J Colloid Interface Sci.* 275: 2 (2004) 360-7. Doi:
466 <https://doi.org/10.1016/j.jcis.2004.02.061>
- 467 [26] A. Hakim, M. Nishiya, M. Kobayashi, Charge reversal of sulfate latex induced by
468 hydrophobic counterion: effects of surface charge density, *Colloid and Polymer*
469 *Science* 294:10 (2016) 1671–1678. Doi: <https://doi.org/10.1007/s00396-016-3931-6>

- 470 [27] M. Ishiguro, W. Tan, L. Koopal, Binding of cationic surfactants to humic substances,
471 Colloids and Surfaces A: Physicochemical and Engineering Aspects 306 (2007) 29–39.
472 Doi: <https://doi.org/10.1016/j.colsurfa.2006.12.024>
- 473 [28] T. Oncsik, A. Desert, G. Trefalt, M. Borkovec, I. Szilagy, Charging and aggregation
474 of latex particles in aqueous solutions of ionic liquids: towards an extended Hofmeister
475 series, Phys. Chem. Chem. Phys. 18 (2016)7511-7520. Doi:
476 [10.1039/C5CP07238G](https://doi.org/10.1039/C5CP07238G)
- 477 [29] A. Martín-Molina, C. Calero, J. Faraudo, M. Quesada-Pérez, A. Travasset, R. Hidalgo-
478 Álvarez, The hydrophobic effect as a driving force for charge inversion in colloids, Soft
479 Matter 5: 7 (2009) 1350. Doi: <https://doi.org/10.1039/b820489f>
- 480 [30] C. Calero, J. Faraudo, Interaction of monovalent ions with hydrophobic and
481 hydrophilic colloids: Charge inversion and ionic specificity, Journal of the American
482 Chemical Society 133:38 (2011) 15025–15035. Doi:<https://doi.org/10.1021/ja204305b>
- 483 [31] W. Xia, Y. Wang, A. Yang, G. Yang, DNA compaction and charge inversion induced
484 by organic monovalent ions, Polymers 9:4 (2017). Doi:
485 <https://doi.org/10.3390/polym9040128>
- 486 [32] R. A. Alvarez-Puebla, J. J. Garrido, Effect of pH on the aggregation of a gray humic
487 acid in colloidal and solid states, Chemosphere 59: 5 (2005)659–667. Doi:
488 <https://doi.org/10.1016/j.chemosphere.2004.10.021>
- 489 [33] U. D. Jovanović, M. M. Marković, S. B. Cupać, Z. P. Tomić, Soil humic acid
490 aggregation by dynamic light scattering and laser Doppler electrophoresis, Journal of
491 Plant Nutrition and Soil Science 176: 5 (2013) 674–679.
492 <https://doi.org/10.1002/jpln.201200346>

- 493 [34] J. A. Molina-Bolívar, J. L. Ortega-Vinuesa, How proteins stabilize colloidal particles
494 by means of hydration forces, *Langmuir* 15: 8 (1999) 2644–2653.
495 <https://doi.org/10.1021/la981445s>
- 496 [35] M. Manciu, E. Ruckenstein, Role of the hydration force in the stability of colloids at
497 high ionic strengths, *Langmuir* 17: 22 (2001) 7061–7070. Doi:
498 <https://doi.org/10.1021/la010741t>
- 499 [36] D. F. Parsons, B. W. Ninham, Charge reversal of surfaces in divalent electrolytes:
500 The role of ionic dispersion interactions, *Langmuir* 26 : 9 (2010) 6430–6436. Doi:
501 <https://doi.org/10.1021/la9041265>
- 502 [37] J. Duan, J. Wang, N. Graham, F. Wilson, Coagulation of humic acid by aluminium
503 sulphate in saline water conditions, *Desalination* 150 : 1 (2002)1–14. Doi:
504 [https://doi.org/10.1016/S0011-9164\(02\)00925-6](https://doi.org/10.1016/S0011-9164(02)00925-6)
- 505 [38] G. Rytwo, Y. Kohavi, I. Botnick, Y. Gonen, Use of CV- and TPP-montmorillonite
506 for the removal of priority pollutants from water, *Applied Clay Science* 36(2007) 182–
507 190
- 508 [39] K. Kawasaki, T. Ebina, T.A. Hanaoka, H. Tsuda, K. Motegi, Heat Resistant
509 Transparent Flexible Film Obtained from Two Tetraphenylphosphonium Modified
510 Smectites with Different Particle Size, *Japanese Journal of Applied Physics* 50 (2011)
511 121601. Doi: 10.1143/JJAP.50.121601
- 512 [40] H. Matsumura, K. Furusawa, Electrical phenomena at the surface of phospholipid
513 membranes relevant to the sorption of ionic compounds. *Advances in colloid and*
514 *interface science* 30 (1989) 71-109
- 515 [41] T. Katsu, H. Nakagawa, K. Yasuda, Interaction between Polyamines and Bacterial
516 Outer Membranes as Investigated with Ion-Selective Electrodes, *Antimicrob Agents*
517 *Chemother* 46 (2002) 1073-1079

- 518 [42] L. Pérez-Fuentes, C. Drummond, J. Faraudo, D. B. Gonzalez, Interaction of organic
519 ions with proteins. *Soft matter* 13 (2017) 1120-1131
- 520 [43] P. Sipos, P. M. May, G. T. Hefter, Carbonate removal from concentrated hydroxide
521 solutions, *Analyst*, 125: 5 (2000) 955–958
- 522 [44] M. L. Jiménez, A.V. Delgado, J. Lyklema, Hydrolysis versus ion correlation models
523 in electrokinetic charge inversion: establishing application ranges, *Langmuir* 28 (2012)
524 6786–6793. Doi:10.1021/la3010773
- 525 [45] H. Hyung, J. H. Kim, Natural organic matter (NOM) adsorption to multi-walled
526 carbon nanotubes: Effect of NOM characteristics and water quality parameters, *Environ*
527 *Sci Technol* 42 (2008) 4416–21. Doi:10.1021/es702916h.
- 528 [46] T. Sugimoto, M. Nishiya, M. Kobayashi, Electrophoretic mobility of carboxyl latex
529 particles: effects of hydrophobic monovalent counter-ions, *Colloid and Polymer*
530 *Science*, Doi : 10.1007/s00396-017-4219-1
- 531 [47] C. Shang, J. A. Rice, Investigation of humate-cetyltrimethylammonium complexes by
532 small-angle X-ray scattering, *Journal of Colloid and Interface Science* 305 (2007) 57-
533 61.
- 534 [48] J. F. L. Duval, K. I. Wilkinson, H. P. Van Leeuwen, J. Buffle, Humic substances are
535 soft and permeable: Evidence from their electrophoretic mobilities, *Environ. Sci.*
536 *Technol.* 39 (2005) 6435–45. Doi:10.1021/es050082x.
- 537 [49] M. J. Avena, K. J. Wilkinson, Disaggregation kinetics of a peat humic acid:
538 mechanism and pH effects, *Environ. Sci. Technol.* 36: 23 (2002) 5100–5105.
- 539 [50] R. L. Wershaw, A new model for humic materials and their interactions with
540 hydrophobic organic chemicals in soil-water or sediment-water system. *Journal of*
541 *Contaminant hydrology* 1(1986) 29-45

- 542 [51] M. Baalousha, F. V. D. Kammer, M. Motelica-Heino, H. S. Hilal, P. Le Coustumer,
543 Size fractionation and characterization of natural colloids by flow-field flow
544 fractionation coupled to multi-angle laser light scattering, *J. Chromatogr. A* 1104
545 (2006a) 272–81. Doi:10.1016/j.chroma.2005.11.095.
- 546 [52] M. Baalousha, M. Motelica-Heino, P. Le Coustumer, Conformation and size of humic
547 substances: Effects of major cation concentration and type, pH, salinity, and residence
548 time, *Colloids Surfaces A: Physicochem. Eng. Asp.* 272 (2006b) 48–55.
549 Doi:10.1016/j.colsurfa.2005.07.010.
- 550 [53] J. Shen, S. Gagliardi, M. R. S. McCoustra, V. Arrighi, Effect of humic substances
551 aggregation on the determination of fluoride in water using an ion selective electrode,
552 *Chemosphere* 159 (2016) 66-71
- 553 [54] L. F. Wang, L-L Wang, X. D Ye, W. W. Li, X. M. Ren, G. P. Sheng, H. Q. Yu, X. K.
554 Wang, Coagulation kinetics of Humic Aggregates in Mono-and Di-valent electrolyte
555 Solutions, *Environ. Sci. Technol.* 47 (2013) 5042-5049.
- 556 [55] J. Gregory, The role of floc density in solid-liquid separation, *Filtration & separation*
557 35 (4) (1998) 367-371.
- 558 [56] D. Wang, R. Wu, Y. Jiang, C. W. K. Chow, Characterization of floc structure and
559 strength: Role of changing shear rates under various coagulation mechanisms, *Colloids*
560 *and Surface A: Physicochemical and Engineering Aspects* 379 (2011) 36-42
- 561 [57] W. Wang, S. Zhao, Q. Yue, B. Gao, W. Song, L. Feng, Purification, Characterization
562 and application of dual coagulants containing chitosan and different Al species in
563 coagulation and ultrafiltration process, *Journal of Environmental Sciences* 51 (2017)
564 214-221
- 565 [58] P. Jarvis, B. Jefferson, S. A. Parsons, Breakage, Regrowth, and Fractal Nature of
566 Natural Organic Matter Flocs, *Environ. Sci. Technol.* 39 (2005) 2307-2314

- 567 [59] M. Kobayashi, Y. Adachi, S. Ooi, On the Steady Shear Viscosity of Coagulated
568 Suspensions, *Nihon Reoroji Gakkaishi* 28(2000)143–144.
569 Doi:10.1678/rheology.28.143.
- 570 [60] H. Amjad, Z. A. Khan, Comparison of Fractal Dimensions of Clay and Humic Acid
571 Flocs under Optimum Coagulation Conditions, *Int J Environ Sci Dev.* 7 (2016), 240–3.
572 Doi:10.7763/IJESD.2016.V7.776.
- 573 [61] C. M. Sorensen, G. M. Wang, Size distribution effect on the power law regime of the
574 structure factor of fractal aggregates, *Physical Review E* 60:6 (1999) 7143-7148
- 575 [62] G. Bushell, R. Amal, J. Raper, The Effect of Polydispersity in Primary Particle Size
576 on Measurement of the Fractal Dimension of Aggregates, *Part. Part. Syst. Charact.*
577 15(1998) 3-8.
- 578 [63] J. E. Martin, Scattering exponents for polydisperse surface and mass fractals, *J. Appl.*
579 *Cryst.* 19 (1986) 25-27.
- 580 [64] L. L. Hoekstra, R. Vreeker, W. G. M. T. Agterof, Aggregation of nickel
581 hydroxycarbonate studied by light scattering, *J Colloid Interface Sci.* 151 (1992) 17-25.
- 582 [65] F. E. Torres, W. B. Russel, W. R. Schowalter, Flocculation structure and Growth Kinetics for
583 rapid shear Coagulation of polystyrene colloids, *J Colloid Interface Sci.* 142 (1991) 554
- 584 [66] H. M. Kwaambwa, M. S. Hellsing, M. J. Wasbrough, M. Bleuel, Salt induced
585 polystyrene latex flocs investigated by neutron scattering, *Journal of Colloid and*
586 *Interface Science* 505 (2017) 9-13.
- 587 [67] M. Kobayashi, S. Ooi, Y. Adachi, On the Yield Stress of Sheared Coagulated
588 Suspensions, *Proc Hydraul Eng* 46 (2002) 637–40. Doi:10.2208/prohe.46.637.

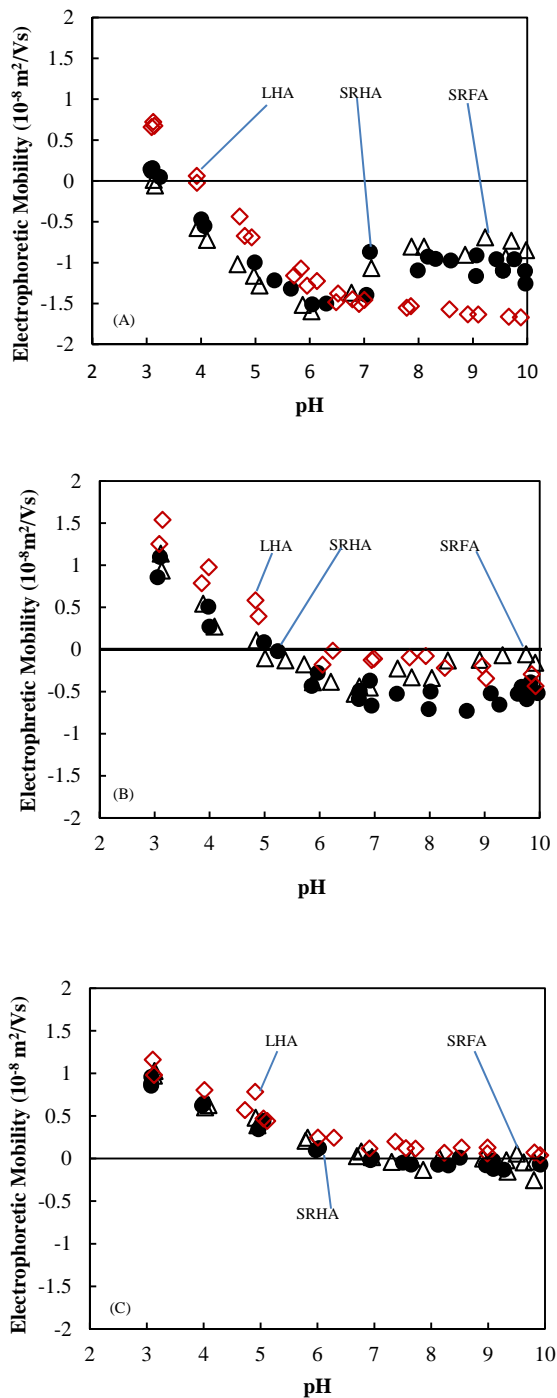
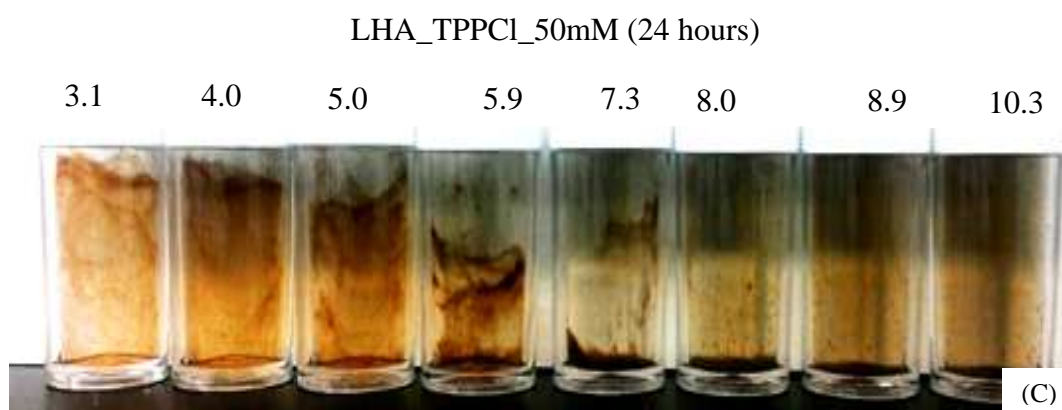
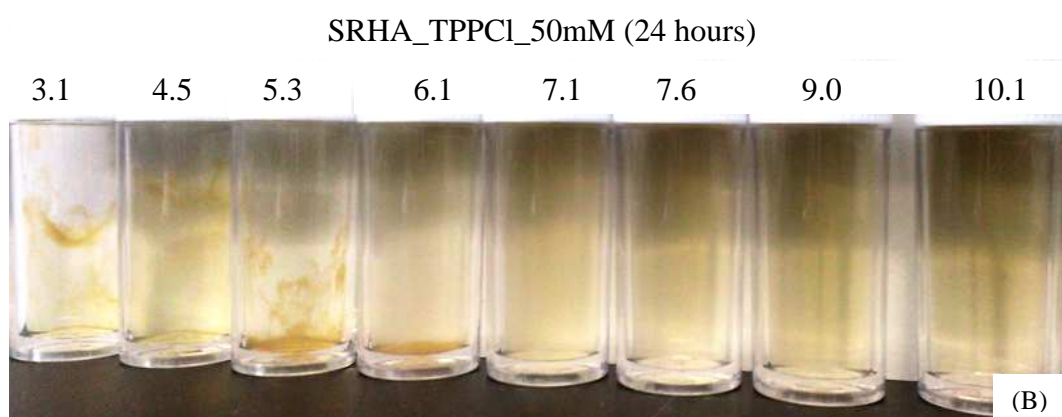
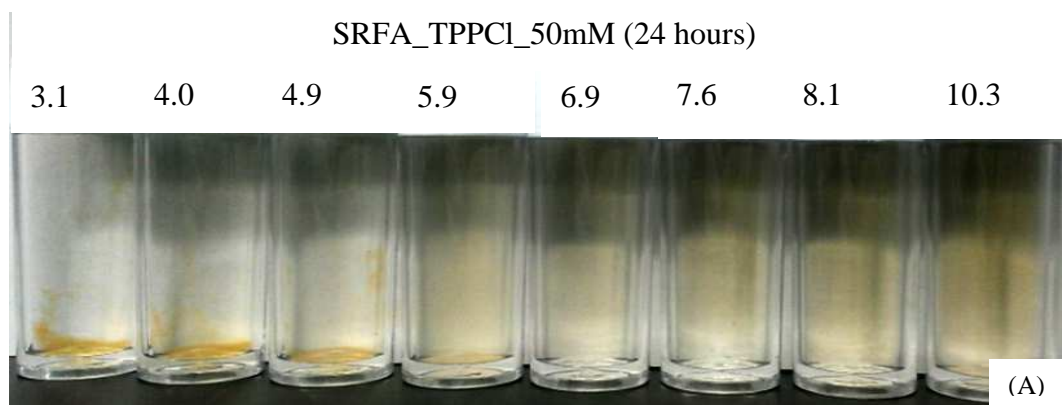
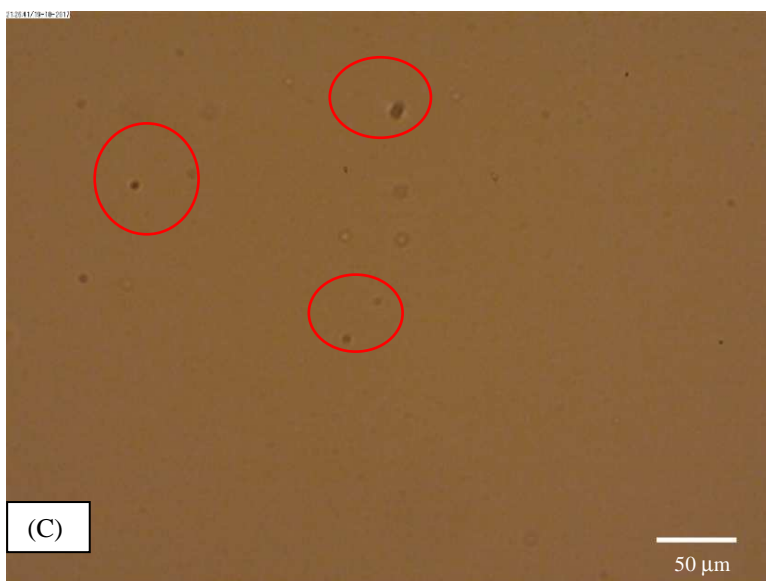
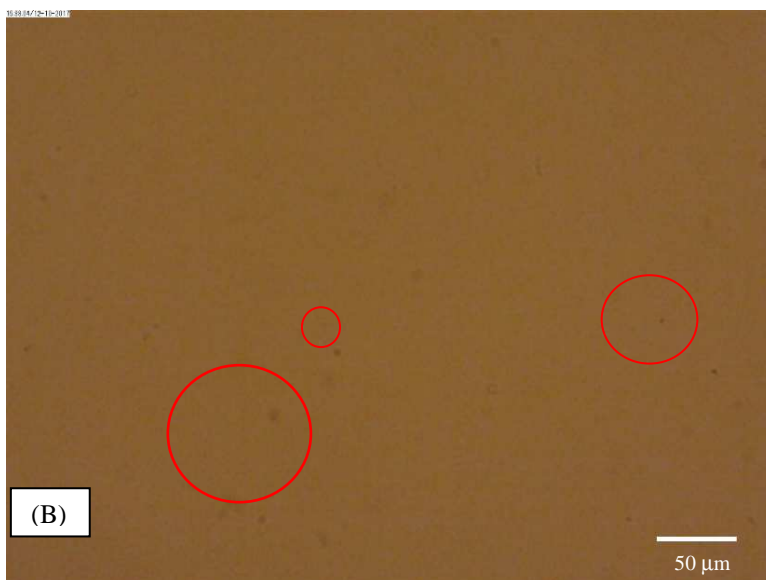
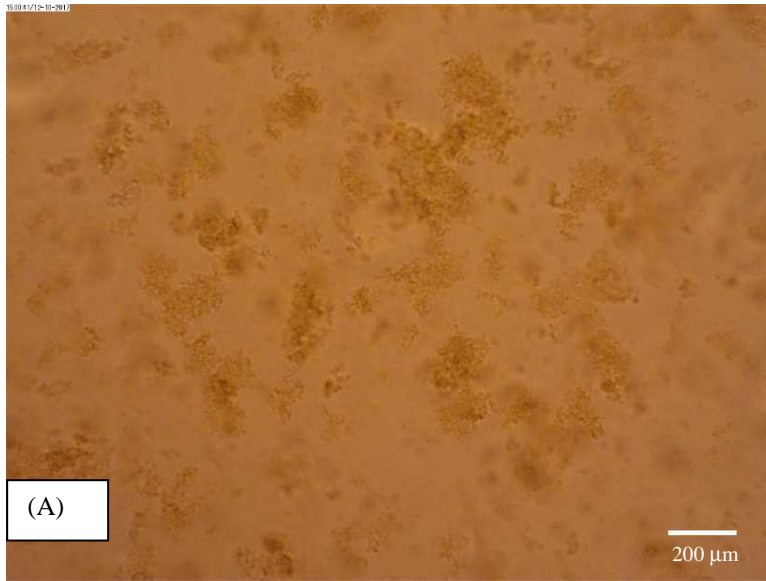


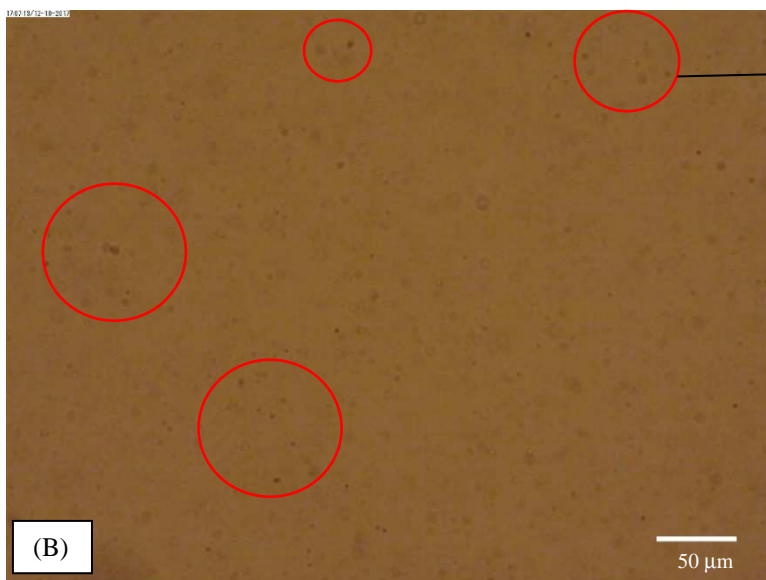
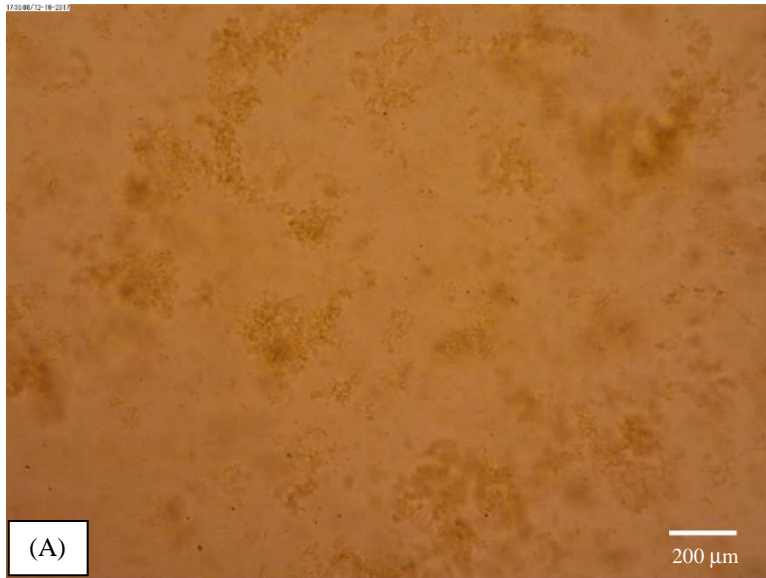
Figure 1. Electrophoretic mobility of Suwanne river fulvic acid (SRFA), Suwannee river humic acid (SRHA) and Leonardite humic acid (LHA) as a function of pH with tetraphenylphosphonium chloride (TPPCL) 10 mM (A), 50 mM (B), and 100 mM (C). Concentration of humic substances (SRFA, SRHA and LHA) is 50 mg/L. Symbols: SRFA (Δ), SRHA (\bullet), and LHA (\diamond).



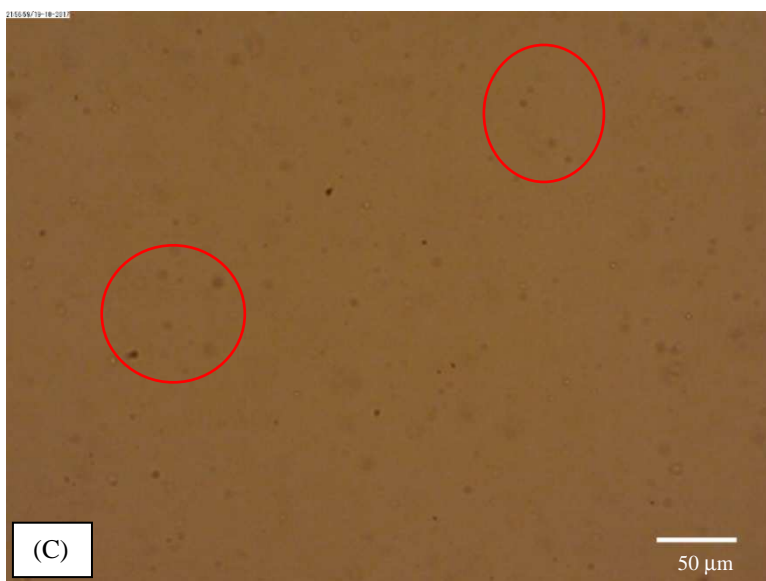
Photograph 1. Macroscopic view of aggregation and re-dispersion for humic substances (SRFA, SRHA, and LHA) in tetraphenylphosphonium chloride (TPPCL) at 50 mM as a function of pH after 24 hours. Photos representing Suwannee river fulvic acid (SRFA) with TPPCl (A), Suwannee river humic acid (SRHA) with TPPCl (B), and Leonardite humic acid (LHA) TPPCl (C). Photo colour was adjusted by using GIMP 2.8.22



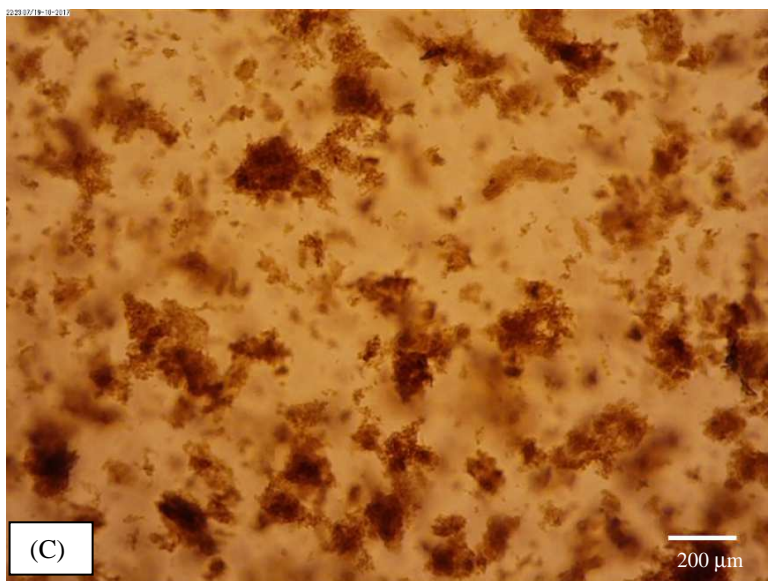
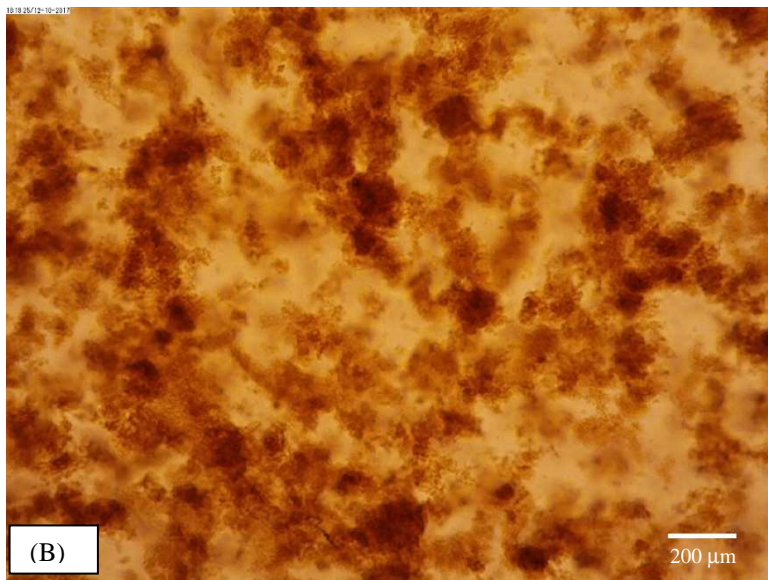
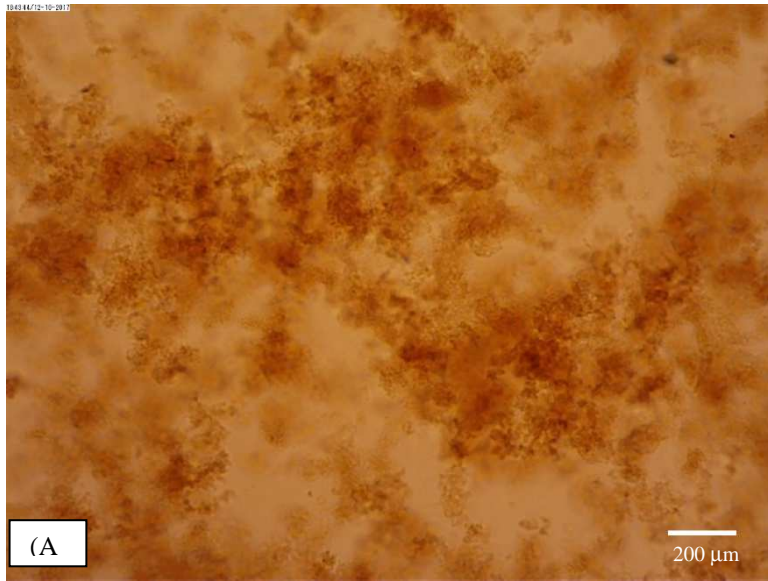
Photograph 2. Microscopic photographs of flocs in Suwannee river fulvic acid (SRFA) with tetraphenylphosphonium chloride (TPPCI) 50 mM at pH 3.1 (A), pH 6.9 (B), and pH 8.9 (C). Scale bar is 200 μm (A), 50 μm (B), and 50 μm (C).



Some small aggregates and particles are dispersed in the suspension. Which indicate the aggregation is induced by tetraphenylphosphonium chloride (TPPCI) at high pH but those are very small in size compared to low pH



Photograph 3. Microscopic photographs of flocs in Suwannee river humic acid (SRHA) with tetraphenylphosphonium chloride (TPPCI) 50 mM at pH 3.2 (A), pH 7.1 (B), and pH 8.8 (C). Scale bar is 200 μm (A), 50 μm (B), and 50 μm (C).



Photograph 4. Microscopic photographs of flocs in Leonardite humic acid (LHA) with tetraphenylphosphonium chloride (TPPCI) 50 mM at pH 3.2 (A), pH 6.8 (B), and pH 8.9 (C). Scale bar is 200 μm .

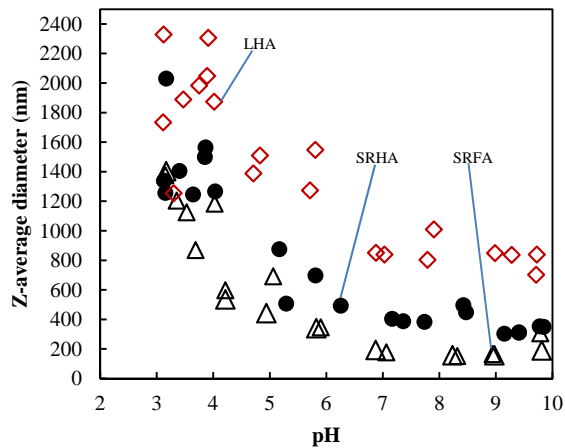


Figure 2. Z average diameter as a function of pH for Suwanne river fulvic acid (SRFA), Suwannee river humic acid (SRHA) and Leonardite humic acid (LHA) in 50 mM tetraphenylphosphonium chloride (TPPCL). Concentration of humic substances (SRFA, SRHA and LHA) is 50 mg/L. Symbols: SRFA (Δ), SRHA (\bullet), and LHA (\diamond).

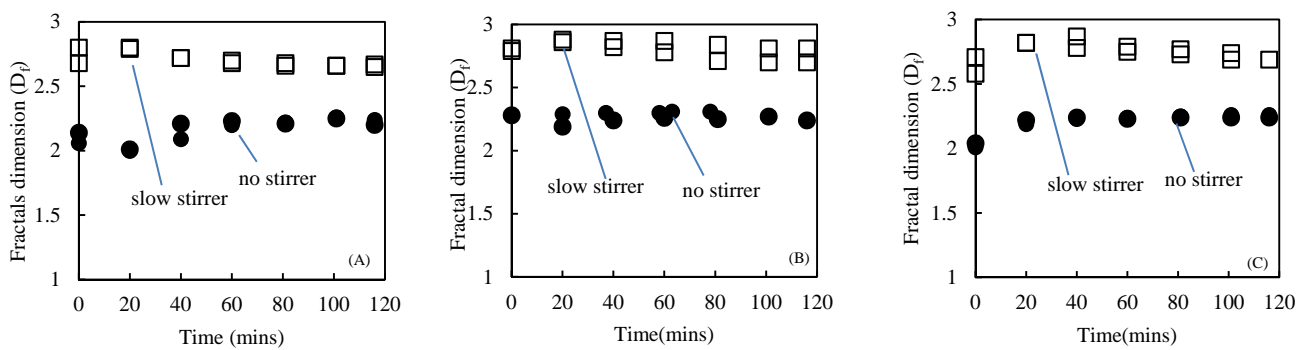


Figure 3. Change in fractal dimension with time in slow stirrer and no stirrer condition of Suwannee river fulvic acid (SRFA) flocs (A), Suwannee river humic acid (SRHA) flocs (B), and Leonardite humic acid (LHA) flocs (C) in 50 mM tetraphenylphosphonium chloride (TPPCL) at pH around 3. Concentration of humic substances (SRFA, SRHA and LHA) is 50 mg/L. Symbols: (\square) slow stirrer, and (\bullet) no stirrer